25th ABCM International Congress of Mechanical Engineering
October 20-25, 2019, Uberlândia, MG, Brazil

COB-2019-0992 STABILITY MAP AND HEIGHTS OF CONFINED INVERSE DIFFUSION FLAMES OF NATURAL GAS AND AIR.

Camilo Andrés Hoyos Álvarez[a].
Paulo R. Pagot[b]
Andrés Armando Mendiburú Zevallos[a].
Fernando Marcelo Pereira[a].
[a]Federal University of Rio Grande do Sul, Av. Paulo Gama, 110, Porto Alegre.
[b]PETROBRAS – Petróleo Brasileiro S.A.
camilo.hoyos@ufrgs.br

Abstract. *Whit the aim to study the behavior of confined inverse flames, an experimental setup is used in which different co-flow conditions of Natural Gas and nitrogen and oxygen mixtures can be tested. Stability regions are determined experimentally. Measurements of the flame height are made through photographic techniques.*

Keywords: *Inverse flame, stability map, confinement.*

1. INTRODUCTION

Inverse diffusive flames IDF are a special case of diffusive flames, in which the fuel and oxidant positions of normal flames NDF are exchanged. Thus, an inverse diffusion flame is formed by the injection of oxidant in a fuel environment. The study of this type of flame is growing due to the advantages it can have over NDFs as a lower production of soot and NOx, and over premixed flames in terms of safety. Further, IDFs are interesting in soot studies. (Makel and Kennedy,2007), (Blevins et al, 2002), (Lee et al, 2005), (Sidebotham and Glassman, 1992), (Escudero et al, 2016).

The reaction in IDFs is dominated by mass diffusion, then, the geometry of the burner nozzle and the flow conditions of the jets modify the degree of fuel and oxidant mixture, which affects the size, anchoring and stability of the flame (Wentzell, 1998). IDFs are generally operated under the buoyancy control due to their relatively small blowout values (Zhu et al, 2019). Thus, it is interesting to study their behavior and stability in different types of burners. One of the most cited works on characterization on laminar inverse flames was made by Wu and Essenhigh (1984) who developed the mapping of the appearance and stability of methane inverse flames, varying the velocities of the concentric jets, in a single jet burner. Choi et al (2015) also presented a turbulent IDF stability map of methane and pure oxygen in a model burner, in which the regions of anchored flames were determined. Sobiesak and Wenzell (2005) analyzed the effect of burner geometry on the behavior of IDF, and presented a stability map of different combinations of fuel and oxidant diameters in concentric co-flow. The results show that in configurations with a low degree of premixing, a balance between the velocities of the two jets is required to maintain the stability of the IDF. High velocities in the oxidant stream and low velocities in the fuel stream cause blowout. Mahesh and mishra (2008) also show stability maps of inverse diffusion flames of liquefied petroleum gas and air (LPG) in a step back burner.

The height of diffusion flames, is a useful parameter in the design of burners and industrial furnaces, and in the improvement of soot production models. Nevertheless, there is no single definition of flame height. Therefore, care should be taken when comparing results and empirical correlations of different authors. The most used definition of flame height is the distance on the center line from the burner tip to the point where the equivalence ratio is unitary. At this point, it is also found the highest temperature of the flame, then it is possible to determine the height of flames through temperature measurements on the center line of the flame. Another technique commonly used to determine the flame height is the approximation of it through direct photographs. This estimate of the height of the flame tends to be greater than the height determined as a function of the stoichiometric ratio or the maximum temperature (Coelho and Costa, 2007).

In IDFs the discrepancy between the definitions of visible height and height based on the mixture fraction, and temperature may be greater, because the soot particle form outside of the flame envelope. Some authors Jung et al (2012), Mikofski et al (2006), Lee et al (2005) have presented IDFs height results measured through OH finding the OH concentration peak, which is near the stoichiometric point.

Others studies Patel and Shah (2018) and Mahesh and Mishra (2010) present results of visible size of IDFs, as a composition of the sum of two heights, the height of the blue zone that is called as premixing height, and the height of area with the highest irradiation called as a luminosity height, associated with soot production. Mikofski et al

(2006) measured heights of the blue zone of methane and ethylene laminar inverse flames through OH-PLIF and compared the results with heights measured as the peak intensity on the center line of the visible image recorded by an ICCD. they found a good agreement between the heights measured by OH PLIF and the heights measured by peak intensity.

Theoretical models for the prediction of the size of diffusive flames have been developed throughout history, Burke-Schumann, (1928) were the first to present an analytical model for this problem. Later some authors have tried to obtain expressions for the height of flame making less simplifications to the problem and expanding their applications. Roper, (1977) presented a modification of the Burke and Schumann theory which considers the variation of the velocity of the jet with the axial distance due to the buoyancy, and proposed models to predict flame heights in circular, square and long slot burners for NDFs. Then, in a second publication Roper et al (1977) they made an experimental verification, and present global correlations that predict the height of NDFs for different fuels. Currently, there are not many publications specifically focused on IDFs height. Wu and Essenhigh (1984) compared IDFs envelopes with relationships based on the work of Gosmann et al (1969) with good agreement, lee et al (2005) compared measured flame height with predicted flame height based on Burke-Schumann theory and Mikofski et al (2006) have made comparisons of experimental data with adaptations of the Roper model for IDFs.

The purposes of this project are, to characterize the appearance and stability of inverse natural gas flames confined in tubes and compare the technique of measuring the height of flames through filtered photographs with experimental data of other authors and the Roper´s model adapted for IDFs.

2. METHOD.

2.1 Experimental setup.

As shown in fig 1, the configuration used to establish the IDFs to be studied in this paper consists of a tube of internal diameter of 7.15 mm, through which the oxidant flows, which is concentrically connected to a square section of 50mm x 50mm, which extends for 500 mm to form a chamber built in stainless steel with two tempered boro-silicate windows for optical access. In the chamber, there is a uniform flow of natural gas. IDF is formed within the chamber, as the central jet of oxidant mixes with the surrounding fuel. An OMEGA pressure transducer (PX119-100AI) is installed on the walls of the square tube to record possible fluctuations that may occur within the chamber due to the presence of the confined flame (Kampen, 2006). Downstream, there is a set of OMEGA type K thermocouples (TJ36- CAIN-18U-6) that record the temperature of the flue gases mixed with the unburned fuel. A SIEMENS (ultramart 23) gas analyzer takes samples of this output mixture and records mole fraction data of CO, NO, SO2, O2, CO2. Finally, the exhaust gases are carried to a ventilation duct, where they are mixed with a large flow of air until they cross the lower flammability limit and are released into the atmosphere.

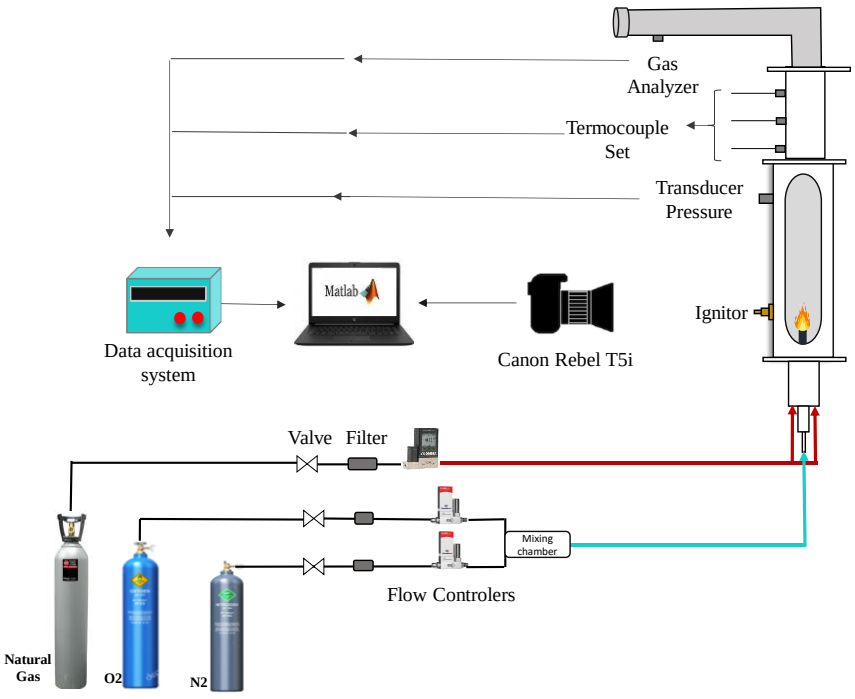

Figure 1. Experimental setup for inverse flame study.

The tests are carried out with commercial natural gas (chemical composition: 90.8% CH4, 6% C2H6, 1.2% C3H8, 0.5% CO2 and 1.55% N2) (Quezada,2017), as fuel and a mixture of nitrogen and oxygen (99% purity). Two BRONKHORST flow controllers (F-201CV-10K) and one OMEGA (FMA-2600A) are used to set the flow rates of N2, O2 and natural gas respectively.

Table 1 lists the flow rates of oxidant and fuel tested. all the flames are in laminar regimen with Reynolds numbers below 400 and Froud numbers less than 1 calculated with the Eq (1). Flames where buoyancy effects are important.

$$Fr = (V_{oxidant}\, Y_{oxidant})^2/(0.6\, g\, H_f\, (T_f/T_\infty)-1)) \quad (1)$$

Where $V_{oxidant}$ is the average velocity of the oxidant at the burner exit, $Y_{oxidant}$ is the mass fraction of the oxidant for complete combustion, T_f is the mean flame temperature, T_∞ is the ambient temperature, g is the gravitational acceleration and H_f *is* the measured flame height. Was taken T_f = 1500 K, which was used by Roper et al (1977).

Table 1. Flow rates for measurements of height flame.

V fuel [1] (m/s)	Q fuel (l/min)	Re fuel [2]	Q air (l/min)	V air [3] (m/s)	Re air [4]
0,07	10	193	1.1	0.46	210
			1.3	0.54	248
			1.5	0,62	286
			1.7	0.71	325
			1.9	0.79	363

[1] V fuel, average fuel velocity at the square tube.
[2] Re fuel, Reynold number of the fuel at the square tube. Hydraulic diameter, Dh= 42mm.
[3] V air, average air velocity at the tube output.
[4] Re air, Reynold number of the air flow at the burner exit. Diameter exit of oxidant, Do= 7.15 mm.

Height measurements of the flame are made through direct photographs using a CCD camera (Canon T5i). The camera stores the output as an RGB image, which is composed by three matrices de m x n elements (pixels), each matrix corresponds to the red, green, and blue intensities of each pixel, on a scale of 0 to 255. The stoichiometric height of the flame was defined as the peak of intensity on the central axis of the flame in the blue channel matrix of the RBG images. The height of the flame is calculated as the average height obtained from a large number of processed photographs, through a two-dimensional pixel coordinate system. A calibration target is used to define the pixel/mm ratio. An analysis of the number of photographs necessary for the convergence of the average flame height is shown in Figure 2. Taking the most extreme case as a global reference, the flame of 1.9 l/min of oxidant. Thus, 60 photographs per flame were defined.

The camera was operated in manual mode by setting the parameters to focal aperture *f/3.5*, exposure time *t/30* s, and sensor sensibility ISO400. The objective of this definition was to capture the greatest amount of light emitted by the flame, blur the background and avoid the appearance of noise in the photographs.

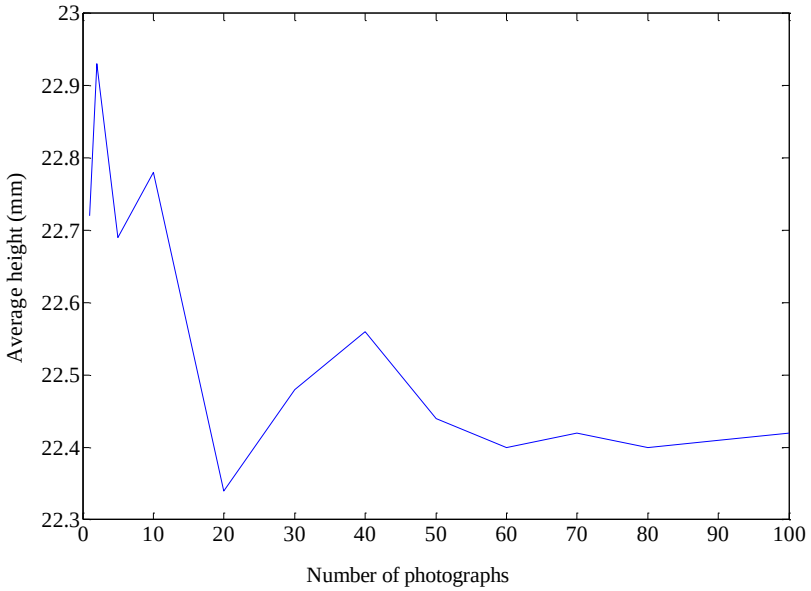

Figure 2. Convergence of the average height flame in relation to the number of photographs (1.9 l/min air flow rate).

2.2 Theoretical analysis.

Theoretical flame height was calculed using the Roper model for circular cross-section burners (Roper, 1977).

$$H_f/Q = [4\pi D_0 Ln(1+1/S)]^{-1}(T_0/T_f)^{0.67} \quad (2)$$

where H_f is the diffusion flame height (cm), Q is the volumetric flow rate of fuel gas corrected to ambient temperature (cm^3/s), D_0 is the diffusion coefficient at ambient temperature (cm^2/s), S the stoichiometric ratio of oxidizer to fuel volume, T_0 is the ambient temperature (K) and T_f is a mean flame temperature (K). In the experimental verification of the model Roper et al (1977) found a linear relationship of the ratio H/Q with the term $[Ln(1+1/S)]^{-1}$ of Eq (2) for different fuels experiments in circular port NDFs. An average value for a proportionality was found, taking T_f and D_0 *as* constants. D_0 was assumed by the authors as the diffusion coefficient of oxygen into nitrogen at ambient temperature ($T_0 = 293$ *K)* calculated from Fristrom et al (1965). And T_f was estimated as 1500K. The resulting the equation is shown below,

$$H/Q = (0.133\ s/cm^2)\ [Ln(1+1/S)]^{-1}. \quad (3)$$

Mikofski et al, (2006) made some modifications of Roper's analysis to use it in IDFs: 1) define Q as oxidant volumetric flow rate and 2) define S as the ratio of fuel to oxidant volume for stoichiometric combustion. Which would be a $S^*=1/S$, (i.e, the reciprocal of the NDF). Initially, they compared OH PLIF measurements of methane and ethylene flame height with Eq (3) adapted for IDFs, and they found discrepancies between the theoretical and experimental data for most of the flames. Then, they optimized the Roper model with experimental data for both methane and ethylene IDFs. The new correlation was better adapted for the methane flames. This suggest that a fuel independent correlation may not exist for IDFs. Finally, an approximation by least squared of the OH PLIF measurements is used to generate a modified Roper's correlation for methane IDF'S. Shown below.

$$H/Q = (0.150\ s/cm^2)\ [Ln(1+1/S^*)]^{-1} \quad (4)$$

3. RESULTS

The map of the flame type and stability region is shown in the figure 3. This graph summarizes the qualitative observations of natural gas IDFs, referring to stability and appearance. Four regions of different velocities ratios were established, boundaries between regions were determined through the observation of changes in the flame, varying the air and fuel flow rates consecutively.

Following 4 flames types may be defined:

- Type I flames: stable, short blue flames that slightly protrude from the tip of the burner. without presence of yellow luminosity.

- Type II flames: stable, blue flames larger than type I with a slight presence of yellow light on the tip of the flame.
- Type III flames: stable, blue flames larger than type I and type II, show more intense yellow luminosity that begins approximately from half the height of the flame.
- Type IV flames: unstable, similar appearance and size as type I, II and III flames in the same air velocity regimes. Apparently sensitive to buoyancy, in some of them there was lift off and subsequent blowout.

In general, variations in the fuel flow rate do not produce significant changes on the appearance and size of the flames. The fuel velocity limit between stability and instability is approximately between (0.3 cm/s - 1 cm/s). Flames of type III are the most large and stable. In this type and in type II, for high fuel velocity, there is presence of flickering. At fuel velocity greater than 50 cm/s it was not possible to stabilize flames due to the large amount of the fuel jet momentum.

It is noted that Figure 3 is similar to the mapping published by Wu and Essenhigh (1984). Although the geometry of the burners is different, the boundaries of the extinction and blowout regions based on the scale of the Reynolds number is very close. Photographs of flame types I, II and III are also shown in Figure 3.

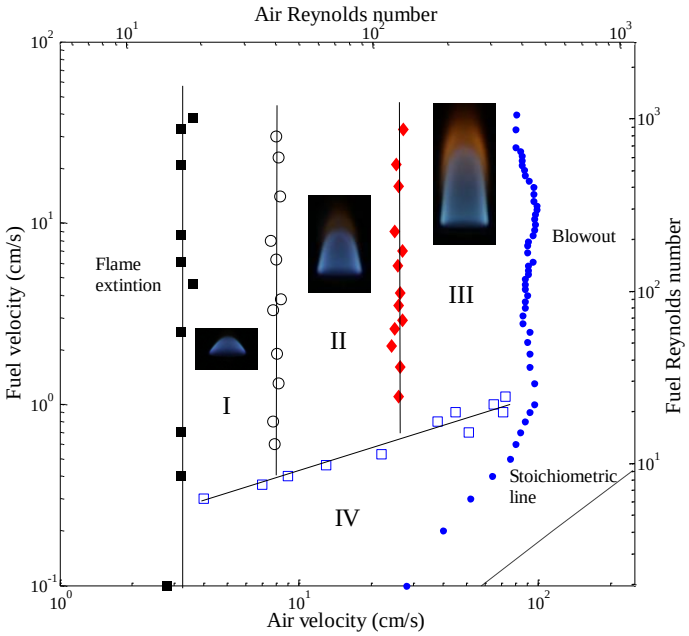

Figure 3. Map of the stability and type of natural gas/air IDF´S.

All height measurements were made on type III flames. A filtered image and a direct photography of a 1.9 l/min air flow rate IDFs is shown in the fig. 4a and 4b respectively. The maximum average intensity peak found in the central axis is shown. Its approximate location is on the parabolic tip of the flame, as expected. This is the area where the reaction rate tends to its highest value and the flame reaches its maximum temperature. It is possible to see that the soot luminosity (orange region) in the direct photograph is very reduced in the filtered image.

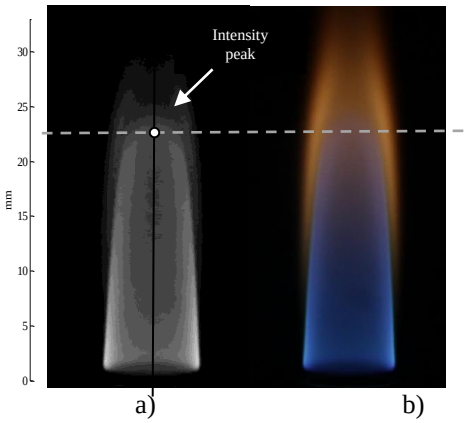

Figure 4. Image of 1.9 l/min air flow rate natural gas IDF a) filtered image b). direct photography.

a) b) c) d) e)

Figure 5. Direct photography on natural gas/air IDFs varying the air flow rate a) 1.1 l/min b) 1.3 l/min c) 1.5 l/min d) 1.7 l/min e) 1.9 l/ min.

Flames images for various air flow rates are shown in fig. 5. The measured flames heights are compared with experimental data of Mikofski et al (2006) in the fig 6. The flame heights measured in this study show a linear increase with the air flow rate, as expected. Flame heights measured by Mikofski et al, (2006) are slightly close to this linear increase for low air flow rates (1.1 l/min to 1.3 l/min). These small differences of height values measured may be due to the slight difference between fuels that modify the value of S* of Eq (4). For higher values of air flow rate (Q > 1.5 l/min) the experimental data of Mikofski et al (2006) changes abruptly and the values move away from the heights measured in this study. This change in the trend of their data does not seem to be related to the measurement method, since the heights measured with OH PLIF stay close to those measured through the peak intensity of the images, regardless the air flow rate. They reported an instability in the flame of 1.6 l/min air flow rate, apparently related to the gas exhaustion system. Which seems to have continued to affect the flames of flow rates above 1.6 l/min.

In the figure 6, can be seen the linear relationship between H and Q of the flames studied in this work, as described in the Roper´s analysis modified for IDFs. However, the proportionality constant between H/Q and $[Ln(1+1/S)]^{-1}$ given by Eq (4) does not fit the trend found. Therefore, the constant for the roper model was adjusted through the linear regression of the experimental data obtained. The resulting correlation is,

$$H/Q = (0.168\ s/cm^2)\ [Ln(1+1/S^*)]^{-1} \quad (5)$$

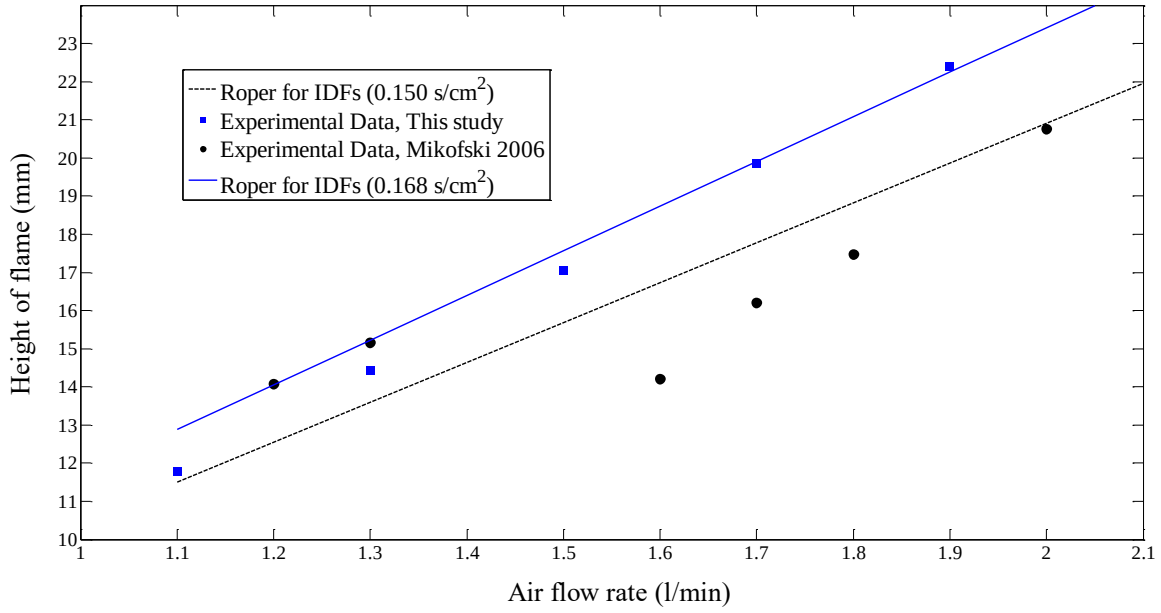

Figure 6. Measured heights of natural gas/air IDFs compared with Roper´s model for NDFs and Roper´s model modified for methane/air IDFs.

4. CONCLUSION

The appearance and stability of inverse laminar flames of natural gas and air were characterized and mapped, these were classified into 4 types by qualitative observation. The results are assimilar to those published by other authors.

Inverse flame heights were measured through photographic techniques for different air flow rates. A linear relationship between the air flow rate and the measured height was observed, in coherence with the Roper model. The measured heights didn´t show the abrupt changes reported by Mikofski et al, (2006). The constant for the Roper´s model was adjusted to the experimental results whit good agreement.

5. ACKNOWLEDGMENTS

The authors are grateful to PETROBRAS – Petroleo Brasileiro S. A. for support of this work through Project PT-143.01.12597 (Sigitec 2017/00622-2).

This study was financed in part by the Coordenação de Aperfeiçoamento de Pessoal de Nível Superior - Brasil (CAPES).

6. REFERENCES

Blevins, L, G; Fletcher, R.A.; Benner, B, A; Steel, E.B; Mulholland, G, W. 2002 “the existence of young soot in the exhaust of inverse diffusion flames” *Proceedings of the Combustion Institute. Volume* 29, pages 2325–2333.

Burke, S.P and Schumann, T. E. W, “Diffusion flames” *Industrial and engineering chemistry.* Vol 20. Page 998

Coelho, P. and Costa, M., 2007. *Combustão*. Edições Orion, Alfragide, 1st edition.

Choi, S, Kim, T, Kim, H, Koo, Kim, J, Kwon, O. “Properties of inverse nonpremixed pure O2/CH4 coflow flames in a model combustor. *Energy.* Vol 93, Pages 1105-1115.

Escudero et al, 2006. “Effects of oxygen index on soot production and temperature in a ethylene inverse diffusion flame”. *Combustion and flames*, Vol. 146, pp. 63–72.

Fristrom, R. M., & Westenberg, A. A. (1965). “Flame structure (Text on flame structure with respect to high-temperature spectroscopy, transport properties, thermodynamics and chemical heat release in gas streams)”. *NEW YORK, MCGRAW-HILL BOOK CO., 1965. 424 P. NAVY-ARPA-ARMY-SUPPORTED RESEARCH.*

Lee, E,J; Oh K.C; Shin, D,H, 2005 “Soot formation in inverse diffusion flames of diluted ethene” *Fuel. Volume* 84, pages 543–550.

Jung et al, 2012. “The effect of oxygen enrichment on incipient soot particles in inverse diffusion flames”. *Fuel*. Vol. 102. Pages 199–207.

Mahesh, S. and mishra, D.P, 2010. “Flame structure of LPG-Air inverse diffusion flames in a back step burner”. *Fuel*, Vol. 89, No. 1, pp. 2145–2148.

Mahesh, S. and mishra, D.P, 2008. “Flame stability and emission cahracteristics of turbulent LPG IDF in a back step burner”. *Fuel*, Vol. 87, No. 1, pp. 2614–2619.

Makel et al, 1994. “Soot Formation in Laminar Inverse Diffusion Flames”. *Combustion science and technology*, Vol. 97:4-6, 303-314.

Mikofski et al, 2006. “Flame height measurement of laminar inverse diffusion flames”. *Combustion and flames*, Vol. 146, pp. 63–72.

Patel, V, Shah, R, 2018 “Experimental investigation on flame appearance and emission characteristics of LPG inverse diffusion flames” *Applied Thermal Engineering.* Elsevier, Vol 137, p. 377-385.

Quezada L.A, 2017, *Experimental study of stability and thermal radiation emission in non-premixed natural gas flames diluted with carbon dioxide*. MSc. dissertation, Federal University of Rio Grande do sul, Porto Alegre, Brazil.

Roper, F. G, 1977. “The prediction of laminar jet diffusion flame size: Part I. Theoretical model. *Combustion and flame.* Vol 29. PP. 219-226.

Roper, F. G, et al 1977. “The prediction of laminar jet diffusion flame size: Part II. Theoretical model. *Combustion and flame.* Vol 29. PP. 227-234.

Sobiesiak, A.; Wenzell J.C. 2005 “Characteristics and structure of inverse flames of natural gas” *Proceedings of the Combustion Institute. Volume* 30, pages 743–749.

Sidebotham, G; Glassman I. 1992 “Flame Temperature, Fuel Structure, and Fuel Concentration Effects on Soot Formation in Inverse Diffusion Flames” *Combustion and flame. Volume* 90, pages 269–283.

Sobiesiak, A., 1998. *Characteristics and Structure of Inverse FIames of Natural Gas*. Ph.D. thesis, Queen's University, Ontario , Canadá.

Wu, K.T; Essenhigh, R.H., 1985. “Mapping and structure of inverse diffusion flames of methane”. *Symposium (International) on Combustion*. Elsevier, vol. 50, p. 1925-1932.

Xuren Z, Xia, X and Zhang, P, 2019 “Stability of Buoyant Inverse Diffusion Methane Flames with Confinement Effects”, Combustion Science and Technology

7. RESPONSIBILITY NOTICE

The authors are the only responsible for the printed material included in this paper.